Thermochimica Acta, 196 (1992) 237–246
Elsevier Science Publishers B.V., Amsterdam

Acoustic emission in the process of dehydration and thermal decomposition of $NaClO_4 \cdot H_2O$

Shiro Shimada

Department of Applied Chemistry, Faculty of Engineering, Hokkaido University, Sapporo 060 (Japan)

(Received 7 July 1991)

Abstract

The dehydration and thermal decomposition of $NaClO_4 \cdot H_2O$ was investigated using a home-made simultaneous AE–DTA apparatus. A sensor with a resonant frequency of 140 kHz, 500 kHz, 1 MHz or 1.5 MHz was used for detecting acoustic emission signals. A wide-band sensor was used for monitoring the power spectra of the signals. Irrespective of the type of reaction holder or the kind of sample, powdered $NaClO_4 \cdot H_2O$ samples give low- and high-temperature AE peaks in the region of 80–310 °C and 450–580 °C, respectively. The high-temperature AE peak consists of six peaks, **a**–**f**. Four peaks, **b**–**e**, are associated with the decomposition of $NaClO_4$, whereas peaks **a** and **f** are due to the melting of $NaClO_4$ and the solidification of molten product NaCl, respectively. The influence of the sample mass and the resonant frequency of the sensor on the low- and high-temperature AE peaks is examined. The power spectra of the signals emitted in peaks **a**–**f** are shown to have their major frequency distribution in a range 80–400 kHz.

INTRODUCTION

Acoustic emission (AE) occurs when the elastic energy accumulated within a stressed body is released because of a dynamic microstructural process such as generation and propagation of cracks or movement of dislocations. Chemical reaction is occasionally followed by mechanical changes in a system containing a solid or liquid (melt) which emits acoustic waves. The AE method, which can detect the acoustic waves, has recently attracted much attention as an interesting technique for chemists. Wentzell and Wade have pointed out the necessity of differentiating between the physical processes occurring in a chemical system by the nature of the acoustic signals emitted, and of examining the characteristics of the power spectra obtained by fast Fourier transform [1].

A previous paper has described a new apparatus for simultaneous measurement of acoustic emission and differential thermal analysis (DTA) and its application to the study of a thermochemical process such as decomposition, dehydration, or phase transition of several solids [2]. It was

demonstrated that the AE technique combined with DTA is a useful, sensitive method for following the process, and for detecting some mechanical changes that could not be distinguished by conventional thermal analysis such as DTA or TG.

Alkali perchlorates are suitable materials for a chemical AE study because they undergo several thermochemical processes of phase transition, melting and decomposition on heating. We have followed the thermochemical processes in $KClO_4$ using the AE–DTA apparatus, and several factors (the particle size and mass, and the nature of the sample) affecting the AE peaks have been examined [3–5]. The thermal decomposition of $NaClO_4 \cdot H_2O$ was briefly studied by the AE–DTA technique [3]; it was reported that on heating, the powdered $NaClO_4 \cdot H_2O$ samples give low- and high-temperature AE peaks in the temperature ranges 80–310°C and 450–580°C, respectively, the latter peak consisting of six peaks. It is necessary to examine how the low- and high-temperature AE peaks are affected by the nature and the amount of the $NaClO_4$ sample and the type of resonance sensor. It is worthwhile investigating the frequency distribution of their signal which could be useful for distinguishing the six peaks and for determining which events may be taking place in the AE peaks. This study reports on the AE peaks occurring during heating of $NaClO_4 \cdot H_2O$ samples and how they are influenced by the nature and mass of the sample, the influence of the resonant frequency of the sensor used; the frequency analysis of the signals is also reported.

EXPERIMENTAL

Two kinds of $NaClO_4 \cdot H_2O$ samples were used (both supplied by Kanto Chem. Co. Ltd., Japan). Using TG, these samples were found to contain approximately one molecular water although they were labelled anhydrous $NaClO_4$. Using an optical microscope, as-received samples can be seen to consist of plate-like or cylindrical agglomerates (100–300 μm) with small particles (30–100 μm). The sample and reference materials were placed in two fused silica holders (15 mm diameter × 15 mm) covered with a cap. A flat-bottomed sample holder (13 mm diameter × 3 mm) without a cap was also used; when this holder was used, the DTA curve cannot be obtained. α-Al_2O_3 powder was used as the reference material. Alumel–chromel thermocouples were used for recording the heating temperature and DTA signal. A heating rate of 5°C min^{-1} was used. A fused silica rod, fixed at the bottom of the sample holder, acts as the waveguide. A piezo-electric sensor resonating at a nominal frequency of 140 kHz, 500 kHz, 1 MHz or 1.5 MHz was attached to the end of rod. The acoustic waves generated in the sample are transmitted through the rod to its end where they are converted by the sensor to electric signals in the form of voltage amplitude–time traces. The traces are passed through a high-pass band filter

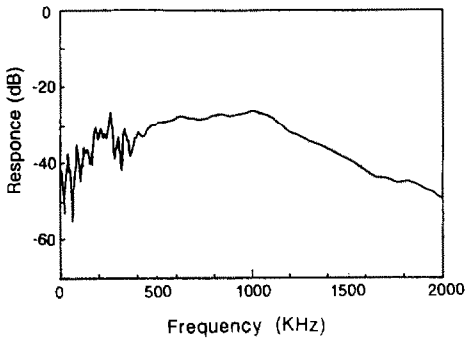

Fig. 1. Frequency response of the wide-band sensor.

with a decaying slope of 18 dB/oct and are discriminated at a pre-set level of voltage, designated the threshold, by an AE tester (NF Electric Instrument, 9501). A threshold value of 250 μV was used unless otherwise noted. The discriminated waves are finally converted to two parameters, the event count rate and the cumulative event count. The time interval of 1 ms is adjusted as a dead time for measurement of an event. The whole AE set-up rests on a non-vibrating base which can diminish mechanical noises from laboratory vibrations. This apparatus was reported in more detail elsewhere [2].

When the power spectra of acoustic emission generated in the $NaClO_4 \cdot H_2O$ samples were recorded, a wide-band AE sensor was used. The frequency response of the sensor is shown to possess a relatively broad band in the range of 300 kHz to 2 MHz (Fig. 1). The signal detected by the sensor is transferred to a digital storage oscilloscope (Iwatsu, Model DS-6411C) on which the corresponding wave form is observed. To monitor a wave, a sampling interval of 200 ns is used, and 1024 points are acquired. 200 waves observed during melting and decomposition were stored on a memory card (Iwatsu, 128 Byte) at a regular time interval of 10–15 s to avoid the intentional sampling of the waves. The digital data of the wave stored are transferred to a personal computer (NEC, PC-9801 type) via a recorder writer (Mitsubishi Plastics, A 0647) and stored on a hard disc as an individual file for later processing. The power spectrum for each wave was calculated with fast Fourier transform (FFT) using the computer.

Using the resonance sensor as a generator, a pulse signal having a nominal frequency of 140 kHz, 500 kHz, 1 MHz or 1.5 MHz was emitted at the inner bottom of the reaction holder toward the end of the waveguide. The transmitted signal was detected by the wide-band sensor and then calculated with FFT. The results are shown in Fig. 2, from which it can be seen that a single peak appears at the corresponding frequency of the pulse signal, indicating that the signals can reach the sensor without changing their frequency components.

RESULTS AND DISCUSSION

Figure 3 (EXP 1 and EXP 2) shows the simultaneous AE–DTA results obtained on heating two kinds of $NaClO_4 \cdot H_2O$, designated K-1 and K-2, respectively. EXP 3 corresponds to the AE result obtained when about a 10 mg cm^{-2} charge of the powdered K-1 sample was thinly spread (about 1 mm thickness) on the flat-bottomed holder. The DTA results (curve A) almost coincide with those reported by Devlin and Herley [6], who showed that the decomposition of $NaClO_4 \cdot H_2O$ is accompanied by four endothermic peaks and one exothermic peak: loss of $0.2H_2O$ at 50–125°C and of $0.8H_2O$ at 155–200°C; phase transition of the orthorhombic to cubic form at 295–315°C; and melting at 485°C, followed by the exothermic decomposition.

No great difference in the AE rate count curves (curve B) for the two samples can be seen. Two main AE features, the low-temperature peak at 80–310°C and the high-temperature peak at 450–580°C, are observed. The thin layer of the sample also produces the low- and high-temperature AE peaks, as shown in Fig. 3 (EXP 3). It is clear that the AE peaks are not greatly influenced by the nature or thickness of the sample, nor by the shape of the holder.

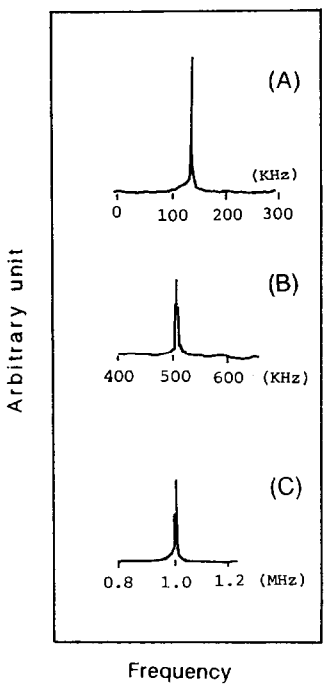

Fig. 2. A peak frequency detected by the wide-band sensor when a pulse frequency of 140 kHz, 500 kHz or 1 MHz is emitted at the bottom of the reaction holder: (A), 140 kHz; (B), 500 kHz; (C), 1 MHz.

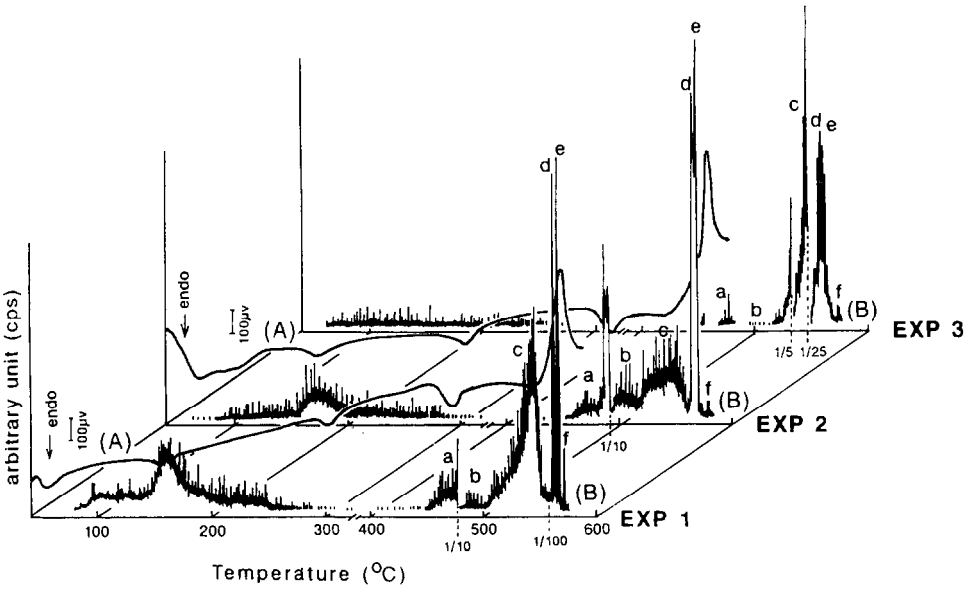

Fig. 3. Simultaneous AE–DTA curves obtained during heating of $NaClO_4 \cdot H_2O$, using two kinds of samples and two types of the reaction holders: EXP 1, K-1 samples (600 mg); EXP 2, K-2 samples (600 mg); EXP 3, K-1 samples (42 mg) using the flat-bottomed holder; (A), DTA curve; (B), count rate curve. Heating rate, 5 °C min^{-1} in air. The threshold is raised at the broken lines, the intensity being reduced to the indicated figures.

As shown in Fig. 3 (EXP 1), the AE signals on the low-temperature peak start at 80°C and intensify with the loss of $0.8H_2O$. Then they continue to appear until the phase transition begins. The AE signals due to the transition are very weak, as compared with the case of $KClO_4$ [4,5]. The high-temperature AE peak gives six peaks (**a**–**f**) above 450°C, which correspond to thermal processes including melting and decomposition. Peak **a** is apparently due to the melting of $NaClO_4$. Because the count rates are higher in peak **b** than in peak **a**, the threshold value had to be raised to 400 μV at 480–490°C, the intensity being reduced to 1/10. Peak **b** begins near the lowest temperature of the endothermic peak due to melting, as observed in Fig. 3, (EXP 1, EXP 2), and continues over the temperature range 480–510°C in which no obvious DTA signal is seen. A simultaneous TG–DTA experiment showed that the weight decrease of $NaClO_4$ begins at the lowest temperature of the endothermic peak, indicating that the evolution of oxygen gas due to the decomposition of $NaClO_4$ begins just after completion of the melting. Peak **b** must be associated with this evolution of oxygen gas. The intense peak **c** appears at 510–560 °C, its later part overlapping with the earlier part of the exothermic DTA peak. Subsequently, two sharp well-resolved peaks **d** and **e** occur at temperatures corresponding to the exothermic peak (peaks **d** and **e** sometimes overlapping with each other). Peaks **c**–**e** are associated with the exothermic peak,

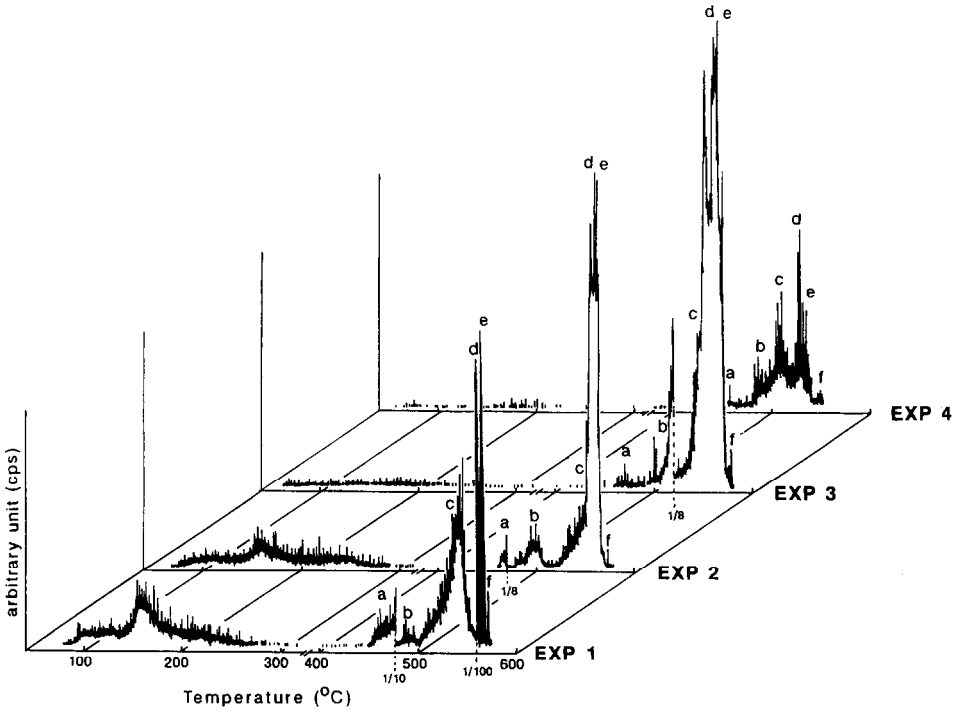

Fig. 4. Influence of the sample amount on the AE peak: EXP 1, 600 mg; EXP 2, 200 mg; EXP 3, 55 mg; EXP 4, 5 mg. The intensity of each AE curve is reduced to the indicated figure by raising the threshold value.

which corresponds to the accelerated weight decrease caused by the oxygen evolution, as seen from the TG–DTA result. Therefore, the decomposition of $NaClO_4$ is believed to consist of four steps corresponding to peaks **b–e**. Peak **f** appears at 570°C at which no DTA signal is observed. This peak is probably due to the solidification of molten product NaCl. Peaks **d–f** were so intense that the threshold value had to be raised again to 500 μV.

Figure 4 shows the effect of the amount of sample on the AE peaks. It is clear that the low-temperature AE peak is reduced by decreasing the sample weight. Because the five high-temperature AE peaks **b–f** are of high intensity for sample weights of 55–600 mg (EXP 1, EXP 2, EXP 3), the pre-selected threshold value had to be raised (see the reduced intensity at the broken line). Peaks **c**, **d** and **e** tend to overlap partially as the sample weight decreases. This overlap is explained by assuming that the mixed high- and low-voltage amplitude–time waves occur at the same time, as reported in a previous paper [4]. The six peaks **a–f** could be measured for a sample as small as 5 mg.

Figure 5 shows the low- and high-temperature AE peaks, including the cumulative count curves, when measured with the four kinds of resonance sensors (140 kHz, 500 kHz, 1 MHz and 1.5 MHz). The AE signals at 1 and

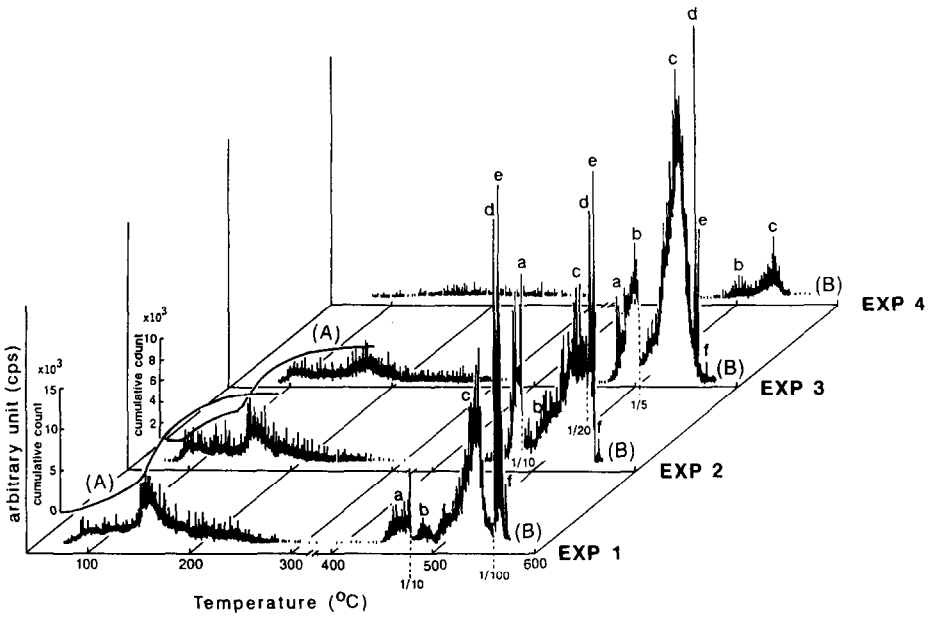

Fig. 5. AE measurement of $NaClO_4 \cdot H_2O$ powders with sensors of different resonant frequencies: EXP 1, 140 kHz; EXP 2, 500 kHz; EXP 3, 1 MHz; EXP 4, 1.5 MHz, (A), cumulative count curve; (B), count rate curve; K-1 samples, 600 mg. Heating rate, 5°C min^{-1} in air. The threshold value is raised at the broken line, the intensity being reduced to the indicated figure.

1.5 MHz were measured at the threshold value of 50 μV. Considering the low threshold value at 1 and 1.5 MHz, the low-temperature AE peak decreases from 140 kHz to 1 MHz, decaying abruptly at 1.5 MHz. The cumulative counts at 500 kHz are two-thirds lower than those at 140 kHz. The AE peak above 260 °C, including the signals due to the structural transition, becomes appreciable at 1 MHz, compared with the case of the dehydration peak. This means that the signals above 260°C have higher frequency components around 1 MHz. The high-temperature AE peak consisting of six peaks also decreases by increasing the resonant frequency of the sensor. Peak **a** becomes weak as the frequency increases to 1 MHz, and is very low at 1.5 MHz. Peaks **b** and **c** still appear even at 1.5 MHz. However, peaks **d** and **e** tend to decay more rapidly in contrast with peaks **b** and **c**, and are finally undetected at 1.5 MHz. Peak **f** shows a gradual decrease with increasing frequency. It is presumed that the process associated with peaks **b** and **c** brings about events with high-frequency components, compared with the process associated with peaks **d** and **e**.

Frequency analysis of the AE signals generated during the melting and decomposition of $NaClO_4$ was performed to obtain their frequency distribution as calculated by FFT (Fig. 6). The interpretation of the spectra is known to be complicated because the acoustic signals generated in a

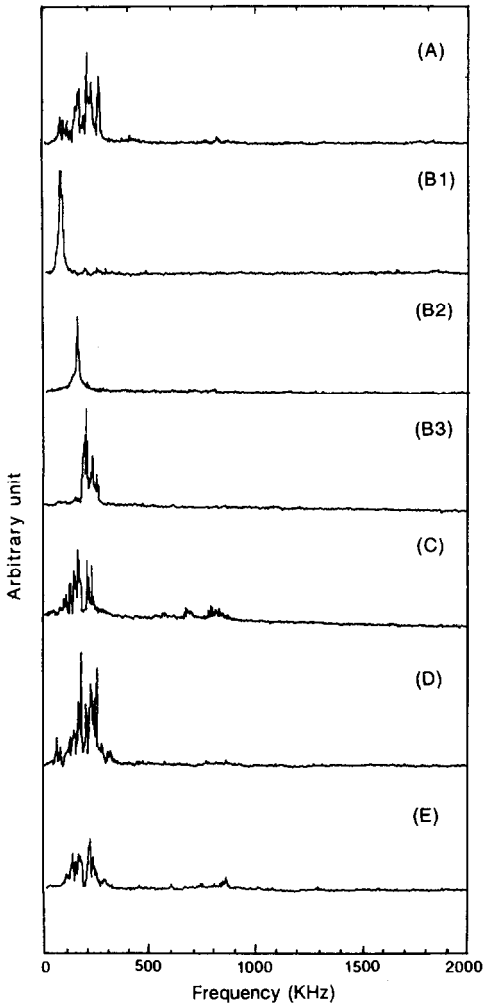

Fig. 6. The frequency distributions of signals emitted at peaks **a–f**: (A), peak **a**; (**B1**) to (**B3**), peak **b**; (C), peak **c**; (D), peak **d**; (E), peak **f**: K-1 samples, 100 mg. Heating rate, 5°C min^{-1} in air.

dynamic system are distorted by several factors [7]. Nevertheless, the frequency spectra appearing in peaks **a–f** should be compared relative to each other rather than absolutely, because the AE signals are transmitted from the waveguide to the sensor without changing their frequency components, as described above (Fig. 2), and are monitored under the same measuring conditions. In order to characterize the spectra, attention was given to their peak frequency.

The spectra in peak **a**, due to the melting of $NaClO_4$ particles, are very complex. They contain frequencies concentrated in the region of 80–300 kHz (Fig. 6(A)), but in rare cases have high-frequency components in the region of 500– 800 kHz. The spectra in peak **b** contain a characteristic

frequency of 80 or 140 kHz, as shown in Fig. 6(B1) and 6(B2), respectively, and show the frequency components in a relatively narrow range of 80–300 kHz (Fig. 6(B3)). In addition, they occasionally have 500–900 kHz frequency components. A single frequency of 80 or 140 kHz suggests a simple event occurring in the molten state. The 80 kHz frequency can probably be attributed to bubble formation [1]. In peak **c**, the spectra show significant contributions at higher frequencies over the broad range of 500 kHz–1 MHz in addition to the major frequencies around 100–400 kHz (Fig. 6(C)). A single frequency of 80 kHz was also observed in the early stage of peak **c**. The spectra in peaks **d** and **e** show complex frequency distributions in a similar way, but contain few frequencies higher than 500 kHz (Fig. 6(D)). Greater contributions at frequencies higher than 500 kHz in peaks **b** and **c** mean that peaks **b** and **c** are still present when a resonant frequency of 1.5 MHz is used (Fig. 5, EXP 4). The spectra in peak **f**, due to the solidification of molten NaCl, are similar to those in peak **c**, having some levels at higher frequencies (Fig. 6(E)). Inspection of the frequency spectra reveals that the six peaks **a–f** are distinguishable from each other. It should be noted that there are strong similarities among the spectra of peaks **b–f**, particularly in possessing the frequency components of 160 and 260 kHz. This suggests that the same mechanical event may continue to occur throughout the decomposition of $NaClO_4$.

The decomposition mechanism of $NaClO_4$ has not been fully understood because of the difficulty in following chemical changes during fusion of the salt by a conventional thermoanalytical or spectroscopic technique. Referring to the papers reported so far [8,9], the decomposition of $NaClO_4$ during fusion can be represented by the overall equations

Major $\quad NaClO_4(s) \rightarrow NaClO_4(l)$ (1)

Minor $\quad NaClO_4(s, l) \rightarrow NaClO_3(l) + 1/2O_2(g)$ (2)

Minor $\quad NaClO_4(s, l) \rightarrow NaCl(l) + 2O_2(g)$ (3)

Minor $\quad NaClO_3(1) \rightarrow NaCl(l) + 3/2O_2(g)$ (4)

These equations are followed by the processes giving rise to the subsequent exothermic eqns. (5)–(7). With rising temperature:

$$NaClO_4(l) \rightarrow NaCl(l) + 2O_2(g) \quad (5)$$

followed by

$$NaClO_4(l) \rightarrow NaCl(s) + 2O_2(g) \quad (6)$$

$$NaCl(l) \rightarrow NaCl(s) \quad (7)$$

each concomitant with eqns. (2) and (4).

It is interesting to consider by reference to the above equations which reactions occur in peaks **a–f**. It was found in our preliminary AE experi-

ments that melts in which no chemical or mechanical dynamic change occurs do not emit any AE. Therefore the AE signals observed above reflect some dynamic chemical change in the melt. Peak **a** results from degradation of particles due to the melting, giving complex spectra as seen in Fig. 6(A). After melting, the signal with a frequency of 80 kHz is often observed in peak **b** and in the early stage of peak **c**. This signal is attributed to bubble formation, which results from release of oxygen gas by a slow decomposition corresponding to the eqns. (2)–(4). With rising temperature, the complicated mechanical events giving complex frequency distributions (Fig. 6(C), 6(D)) continue to take place in peaks **c**–**e**. The higher counting rates in peaks **c**–**e** suggest rapid out-gassing of oxygen or bumping, according to eqns. (5) and (6). Peak **c** contains higher frequency components in the region of 500–800 kHz than peaks **d** and **e**. The origin of these components is not clear at present. The molten NaCl begins to solidify with rather complex frequency distributions near the end of the exothermic peak, as seen in Fig. 6(E).

REFERENCES

1 P.D. Wentzell and A.P. Wade, Anal. Chem., 61 (1989) 2638.
2 S. Shimada and R. Furuichi, Bull. Chem. Soc. Jpn., 63 (1990) 2526.
3 S. Shimada and R. Furuichi, Thermochim. Acta, 163 (1990) 313.
4 S. Shimada, Y. Katsuda and R. Furuichi, Thermochim. Acta, 183 (1991) 365.
5 S. Shimada, Y. Katsuda, R. Furuichi and M. Inagaki, Thermochim. Acta, 184 (1991) 91.
6 D.J. Devlin and P.J. Herley, React. Solids, 3 (1987) 75.
7 M. Ohtsu, The Characteristics and Theory of Acoustic Emission, Morikita Pub. Co., Tokyo, 1988, p. 54, in Japanese.
8 M.M. Markowitz and D.A. Boryta, J. Phys. Chem., 69 (1965) 1114.
9 H.F. Cordes and S.R. Smith, J. Phys. Chem., 72 (1968) 2189.